ATATÜRK ÜNİVERSİTESİ YAYINLARI
ATATURK UNIVERSITY PUBLICATIONS

Research Article *Araştırma Makalesi* DOI: 10.16951/trendbusecon.2001615

Segmented or Integrated? Volatility Connectedness Between Commodity Futures and Cryptocurrencies

Ayrışık mı, Bütünleşik mi? Emtia Vadelileri ile Kripto Paralar Arasında Oynaklık Bağlanmışlığı

Yusuf AKGÜL
Department of International Trade and Logistics, Sivas Cumhuriyet University, Faculty of Economics and Administrative Sciences, Sivas, Türkiye

ABSTRACT

This study examines whether commodity futures and cryptocurrency markets constitute a single integrated risk system or remain largely segmented in terms of volatility. Using daily data on six commodity futures contracts (gold, silver, copper, WTI crude oil, natural gas, wheat) and four cryptocurrencies (Bitcoin, Ethereum, XRP, Litecoin) over 25 August 2016 – 30 June 2026 (2,471 trading days), conditional volatilities estimated by GARCH(1.1) are embedded in a ten-variable VAR, and spillovers are measured with the Diebold–Yılmaz connectedness framework. The central contribution decomposes total connectedness into within-block and cross-block components, complemented by DCC-GARCH return correlations. Total connectedness is 28.7%, yet 61.4% occurs within the crypto block and 34.9% within the commodity block, leaving only 3.6% to cross-block transmission. Natural gas (+20.4) and Ethereum (+8.5) are the leading net transmitters and gold the largest net receiver (−18.7). Commodity–crypto correlations remain low and inert (0.040–0.123), and the segmentation is robust to the forecast horizon, VAR lag length, window width, return frequency, volatility measure, sample period and data source. The findings indicate distinct shock sources and durable diversification; aggregate connectedness can conceal block structure.

JEL Codes: C58, G11, G15, Q02

Keywords: Volatility Connectedness, Diebold–Yılmaz, DCC-GARCH, Cryptocurrency, Commodity Futures

ÖZ

Bu çalışma, emtia vadeli işlem piyasaları ile kripto para piyasalarının oynaklık bakımından tek bir bütünleşik risk sistemi mi oluşturduğunu yoksa büyük ölçüde ayrışık mı kaldığını incelemektedir. 25 Ağustos 2016 – 30 Haziran 2026 dönemine ait günlük verilerle (2.471 ortak işlem günü) altı emtia vadeli işlem sözleşmesi (altın, gümüş, bakır, WTI ham petrol, doğal gaz, buğday) ve dört kripto para (Bitcoin, Ethereum, XRP, Litecoin) için GARCH(1,1) ile tahmin edilen koşullu oynaklıklar on değişkenli bir VAR sistemine yerleştirilmiş ve yayılımlar Diebold–Yılmaz bağlanmışlık çerçevesiyle ölçülmüştür. Çalışmanın temel katkısı, toplam bağlanmışlığın blok-içi ve bloklar-arası bileşenlerine ayrıştırılması ve bulguların DCC-GARCH korelasyonlarıyla getiri düzeyinde desteklenmesidir. Sistemin toplam bağlanmışlığı %28,7'dir; ancak bunun %61,4'ü kripto, %34,9'u emtia bloğunun kendi içinde gerçekleşmekte, çapraz yayılıma yalnızca %3,6 kalmaktadır. Başlıca net yayıcılar doğal gaz (+20,4) ve Ethereum (+8,5), en büyük net alıcı ise altındır (−18,7). Emtia–kripto korelasyonları düşük ve istikrarlı kalmakta (0,040–0,123); ayrışma bulgusu öngörü ufkuna, VAR gecikme uzunluğuna, kayan pencere genişliğine, getiri frekansına, oynaklık ölçütüne, alt döneme ve veri kaynağına karşı dayanıklıdır. Bulgular, iki piyasanın farklı şok kaynaklarınca sürüklendiğini ve kalıcı çeşitlendirme sağladığını; toplam bağlanmışlık ölçütlerinin blok yapısını gizleyebildiğini göstermektedir.

JEL Kodları: C58, G11, G15, Q02

Anahtar Kelimeler: Oynaklık Bağlanmışlığı, Diebold–Yılmaz, DCC-GARCH, Kripto Para, Emtia Vadelileri

Geliş Tarihi/Received 23.07.2026
Kabul Tarihi/Accepted 11.10.2026
Yayın Tarihi/Publication Date 15.10.2026

Sorumlu Yazar/Corresponding author: Yusuf AKGÜL
E-mail: yusufakgul@cumhuriyet.edu.tr
Cite this article: Akgül, Y. (2026). Segmented or Integrated? Volatility Connectedness between Commodity Futures and Cryptocurrencies. *Trends in Business and Economics*, *40*(4), 776-796.

Content of this journal is licensed under a Creative Commons Attribution 4.0 International License

Introduction

The growing integration of financial markets has turned the understanding of risk transmission channels across asset classes in particular into a central question for both portfolio management and systemic risk oversight. The extent and speed with which uncertainty arising in one market is transmitted to another determine the true limits of diversification. Indeed, the tightening of cross-asset linkages precisely when diversification is needed most, in periods of stress, has been documented as one of the most fragile points of portfolio theory (Page & Panariello, 2018).

Commodity futures markets have interacted ever more intensively with traditional asset classes since the financialization process that began in the 2000s; while they continue to serve as instruments through which producers and industrial users manage price risk, they have also become a distinct asset class for institutional investors (Erb & Harvey, 2006; Gorton & Rouwenhorst, 2006; Levine et al., 2018). This transformation has heightened the sensitivity of commodity returns to macroeconomic news flow and financial market conditions (Hess et al., 2008), and has placed the volatility linkages of commodity groups both among themselves and with outside markets on a new research agenda.

Over the past decade, cryptocurrencies have emerged as a third asset class, marked by high volatility, rapidly growing market capitalization and increasingly institutionalized trading infrastructures (Hornback & Whaley, 2025; Krückeberg & Scholz, 2020). Although the regulatory framework and market integrity of crypto assets remain contested (Edwards et al., 2019), their derivative markets have deepened rapidly (Dutta, 2025; Lupu & Popa, 2024) and their share in institutional portfolios has grown. This development raises a natural question: are commodity futures markets and cryptocurrency markets parts of a single integrated risk system in terms of volatility, or do they form two largely segmented islands?

This question is not merely a matter of academic curiosity. If the two markets are integrated, adding crypto assets to commodity portfolios will forfeit its apparent diversification benefit in times of crisis, and systemic risk oversight will require the two markets to be monitored jointly. If they are segmented, crypto assets will offer commodity portfolios a genuine and durable source of diversification; yet this would also imply that the two markets are driven by independent sources of shocks that do not propagate from one to the other.

The volatility spillover literature commonly addresses such questions with the vector autoregression (VAR) based connectedness framework of Diebold and Yilmaz (2012). Built on the generalized forecast error variance decomposition, this approach makes it possible to measure each asset's contribution to the volatility uncertainty of the others and thereby to map risk transmission at the total, directional and pairwise levels. The framework has found a wide range of applications, from measuring tail risk spillovers in commodity futures markets (Ren et al., 2025) and tracking global commodity shocks (Wang et al., 2026), to uncovering the hierarchical structure of currency networks (Li et al., 2026) and examining the time frequency linkages between tokenized and traditional derivatives (Abdullah et al., 2026). By contrast, a comprehensive treatment of volatility spillovers between commodity and cryptocurrency markets that combines both groups within a single system and decomposes connectedness at the block level remains relatively scarce.

This study combines six commodity futures contracts (gold, silver, copper, WTI crude oil, natural gas, wheat) and four cryptocurrencies (Bitcoin, Ethereum, XRP, Litecoin) in a single ten-variable connectedness system and investigates four questions: (i) what is the level of total and directional (net) volatility connectedness in the system; (ii) how large is the mutual spillover between the commodity and crypto blocks relative to the spillover within each block; (iii) how does connectedness evolve over time, and how does it behave during crisis episodes; (iv) do pairwise dynamic correlations corroborate this picture?

The study makes three contributions to literature. The first is to decompose total connectedness at the block level, showing quantitatively that cross-market spillover accounts for less than four per cent of the total; the conclusion one would draw from the headline connectedness figure that "the system is moderately integrated" is shown to conceal a concentration of spillovers within blocks. Second, the robustness of this segmentation to the forecast horizon, the VAR lag length, the rolling window width, the return frequency, the volatility measure, the sample period and the choice of data vendor is examined through a systematic sensitivity analysis. Third, the volatility-based findings are complemented by dynamic conditional correlations of return shocks, which point to the same conclusion at the return level.

The remainder of the paper presents the conceptual

framework and the related literature, describes the data and methodology, reports the empirical findings together with further robustness and diagnostic analyses, and concludes with a discussion, implications and suggestions for future research.

Conceptual Framework and Literature

Volatility, connectedness and spillovers: conceptual foundations

The concept of volatility spillover rests on the idea that uncertainty in one market has predictive power for uncertainty in another. This is distinct from causality at the level of the mean (returns): even if the returns of two assets are uncorrelated, their volatilities may feed each other. Spillovers typically originate from common information flows, a shared investor base, liquidity constraints and portfolio rebalancing behavior. In commodity markets, these channels are supplemented by storage and supply constraints, convenience yield dynamics and movements in the term structure (Nakajima, 2020).

The conceptual core of connectedness measurement is the share of an asset's forecast error variance explained by its own shocks versus the shocks of the other assets (Diebold & Yilmaz, 2009). The magnitude of the off-diagonal shares gives the degree of integration of the system. This measurement combines naturally with network theory: each asset can be interpreted as a node and each directional share as an edge, so that net transmitters and net receivers can be distinguished. Studies that examine the network structure of futures markets directly support this view: Wu et al. (2015) transformed index futures price series into a complex network and showed that the degree distribution follows a power law, while Abideen and Wu (2026) developed a network-based stochastic volatility model that embeds the network Laplacian into the volatility dynamics, showing that sparse and dense network structures amplify volatility clustering differently. Connectedness is thus not merely an aggregate metric but a matter of topology, which justifies the examination of block structure.

The time scale of measurement also matters. Bartolozzi et al. (2007) documented, using high-frequency data from several futures markets, that correlations display a multi-scale structure, suggesting that connectedness measured at a single horizon may give only a partial picture; this motivates the sensitivity analysis of the forecast horizon reported below.

In this study, connectedness is built on conditional volatilities rather than returns. The reason is conceptual: the object of interest is the transmission of risk, not the transmission of mean returns. Estimating conditional volatility with univariate GARCH models and then feeding it into a multivariate system is a well-established practice in the commodity volatility literature (Clewlow et al., 2014).

Volatility spillovers in commodity markets

Volatility transmission across commodity groups has been widely documented. Grieb (2015) demonstrated mean and volatility transmission among commodity futures within a multivariate GARCH framework, and Sayed and Auret (2019) found significant volatility spillovers in the futures markets of major maize exporters. Rezitis et al. (2024) showed that the linkages between energy and agricultural futures are asymmetric and regime-dependent, with cross-correlations rising in high-volatility regimes.

Applications of the Diebold–Yılmaz framework to commodities have diversified in recent years. Ren et al. (2025) extended the connectedness network of commodity futures with a bootstrap-based approach to measure tail risk connectedness, while Wang et al. (2026) documented global commodity spillovers under VIX shocks using a dynamic quantile network model. Qin and Lau (2024) showed that quantile-based extreme risk spillovers from U.S. soybean futures to China's soybean-linked futures markets are time-varying and asymmetric, and Zhou and Li (2026), studying the contagion of commodity futures price bubbles with a time-varying parameter connectedness model, documented that sentiment contagion markedly amplifies bubble contagion in the short run and switches sign during crises such as COVID-19.

The scope of spillover analysis has also expanded beyond commodities. Moutinho et al. (2026) examined risk transmission between financial markets (G7 and Chinese indices) and commodity markets (gold and oil) during COVID-19 within a DCC-MGARCH and conditional value-at-risk framework, finding that oil carried the highest risk exposure while gold generally behaved as a safe haven. In the context of climate markets, Hoque et al. (2023) documented one-way, positive volatility spillovers from carbon futures to climate change futures, and Liu et al. (2026) forecast extreme downside risk spillovers between carbon and energy markets with quantile machine learning. Collectively, these findings indicate that

the commodity block is meaningfully connected both internally and with neighboring markets.

Crypto assets: a new asset class and its volatility structure

The volatility structure of cryptocurrency markets differs markedly from that of traditional assets, and no consensus has yet formed on their relationships with traditional asset classes. Krückeberg and Scholz (2020) documented the existence of arbitrage opportunities in Bitcoin markets and the limits of market efficiency, and Conlon et al. (2024) related Bitcoin basis risk to investor sentiment and unexpected inflation.

The microstructure of crypto derivative markets has also been researched intensively. Frino et al. (2025) showed that the distribution of Bitcoin price discovery between spot and futures markets remains unsettled; Chen and Yang (2024) documented that, for two Bitcoin futures contracts of different sizes written on the same underlying, price discovery depends on relative liquidity and investor composition. Shynkevich (2026) found periodic patterns of algorithmic trading origin at sub-second frequencies in the spot and perpetual futures markets of Bitcoin and Ethereum, showing that these periodic jumps increase volatility and transaction costs. Dutta (2025) assessed the risk structure of the Bitcoin futures market, and Lupu and Popa (2024) examined the efficiency of cryptocurrency futures markets. Hornback and Whaley (2025) evaluated the approval process and market impact of spot Bitcoin exchange-traded funds, highlighting a turning point in the institutionalization of crypto assets.

The distributional properties of crypto returns are particularly relevant for the diagnostic findings of this study. Karagiorgis and Ballis (2026) found a strong convex relationship between skewness and kurtosis in Bitcoin spot and futures markets and showed that higher moments vary markedly over time; this indicates that crypto volatility is not merely high but also driven by extreme events.

The regulatory and market integrity dimension of crypto assets is likewise an active area of debate. Edwards et al. (2019) argued that crypto assets require better regulation, and Yang and Kwon (2026) predicted exchange delisting events with explainable machine learning, documenting the idiosyncratic institutional risks of these markets. Connectedness within the crypto universe itself has also been measured: Khan et al. (2026) examined the connectedness across healthcare cryptocurrencies, decentralized finance (DeFi) indices and non-fungible tokens with a time-varying parameter VAR, showing that DeFi is the dominant net transmitter. Korolev (2026), in turn, documented that decentralized finance assets exhibit limited correlation with traditional assets. Taken together, these findings suggest that the crypto block may be densely connected internally while only weakly linked to the outside.

Market segmentation, integration and diversification

The central prediction of diversification theory is that holding assets with low correlations reduces portfolio risk. The weakest point of this prediction in practice, however, is that correlations are not constant. Page and Panariello (2018) showed that diversification fails precisely in the down-market conditions in which it is needed most, with correlations rising systematically during periods of stress. Diversification claims should therefore be tested not only with unconditional correlations but with time-varying and regime-sensitive measures.

The literature on co-movement and contagion across futures markets supports this caution. Pan and Hsueh (1998) found one-way return and volatility spillovers between the U.S. and Japanese index futures markets, with the U.S. influence roughly four times as large as that in the reverse direction. Albulescu et al. (2017) documented that the co-movement among six international index futures markets becomes pronounced especially in the long run and that rolling wavelet correlations rise after turbulence episodes. Wong et al. (2007) showed that volatility in real estate spot and forward markets is transmitted predominantly from the forward market to the spot market, establishing that the direction of spillovers depends on market structure. In the context of the fragility of financial networks, Getmansky et al. (2016) measured the interconnectedness of the credit default swap market and drew attention to the systemic risk carried by dense linkages.

The diversification benefits of commodity futures have also been studied extensively. Demiralay et al. (2019) measured the time-varying diversification benefits of commodity futures with dynamic correlation models, and Demiralay et al. (2025) showed how stock–commodity correlations evolve with climate risks and what this implies for optimal hedging. Zainudin and Mohamad (2023) documented that the co-movement of global futures markets increased during the pandemic and that this affected hedging effectiveness.

Studies that consider commodities and crypto assets jointly are comparatively recent. Abdullah et al. (2026)

examined the tail risk connectedness between tokenized and traditional derivatives in a time–frequency framework and offered portfolio implications. The present study advances this line of research by combining commodity futures and cryptocurrencies in a single system and measuring block spillovers directly.

Dynamic correlation and portfolio implications

Connectedness measures the linkages of the system in the volatility dimension; for portfolio construction, however, the evolution of return correlations over time is also decisive. Dynamic conditional correlation (DCC) models provide a parsimonious way of estimating the time-varying structure of conditional correlations and are widely used in the commodity context (Demiralay et al., 2019; Rezitis et al., 2024). In this study, DCC provides complementary evidence at the level of return co-movement: connectedness is measured on conditional volatilities (the second moment), whereas DCC captures the time-varying correlation of standardised return shocks (the first moment), so that agreement between the two measures is informative rather than mechanical.

As regards tail risk and extreme events, van Oordt et al. (2021) established within an extreme value theory framework that agricultural commodities are heavy-tailed; Niu et al. (2024) showed that gold market volatility can be predicted by speculation and cross-market sentiment; and Jensen et al. (2018) questioned widely held beliefs about the role of gold within portfolios. Sharma and Karmakar (2024) demonstrated the impact of asymptotic tail dependence on hedging effectiveness, cautioning that central correlation measures may fail to represent tail behaviour. The general investment character of commodity markets and their financialisation were established by Gorton and Rouwenhorst (2006) and Erb and Harvey (2006); the sensitivity of commodity futures to macroeconomic news was documented by Hess et al. (2008), the role of speculative trading activity by Chen and Yu (2025), and the explanatory power of news-based information flows in the oil market by Calomiris et al. (2026). Etienne et al. (2025) decomposed commodity risk premia into common and idiosyncratic components, pointing to the existence of a common systematic factor across commodities a finding directly related to the within-block concentration result of this study.

Data and Methodology

Data

The study uses daily closing prices for the period 25 August 2016 – 30 June 2026; all prices are denominated in US dollars. The system consists of ten assets: six commodity futures contracts (gold, silver, copper, WTI crude oil, natural gas, wheat) and four cryptocurrencies (Bitcoin, Ethereum, XRP, Litecoin). The commodities were selected so as to represent the three main groups (precious metals, base metals, energy) as well as agricultural products; the cryptocurrencies were chosen to cover the dominant assets by market capitalization and trading volume.

Gold and silver futures prices were obtained from Yahoo Finance (continuous nearest-contract series, symbols GC=F and SI=F); the remaining four commodity series and the four cryptocurrency series were obtained through an official subscription to investing.com. In addition, Microsoft Excel and Python were used to implement methodologies.

The series were matched on common trading days (inner join) and missing observations were excluded. Because cryptocurrencies trade on weekends whereas commodity futures do not, the common calendar intersection was used; the final sample comprises 2,471 common trading-day observations. This matching implies that weekend cryptocurrency movements are absorbed into the first common observation of the following week.

One property of the commodity series requires explicit disclosure: they are continuous nearest-contract futures prices that are not back-adjusted at contract rolls, so a roll date can produce a large return that is reversed shortly afterwards (Carchano & Pardo, 2009); the April 2020 WTI observations and the January 2026 natural gas observation are of this type. The common calendar itself is regular: all five weekdays are represented (497 Friday observations), the sample contains approximately 251 observations per year, and only 2.9% of the returns span an interval longer than a weekend, reflecting exchange holidays. A 250-observation window therefore corresponds to about one trading year.

Throughout the paper, ‘daily’ refers to returns between consecutive observations of the common calendar. Because that calendar covers all five weekdays, one observation corresponds to one trading day, and window and horizon lengths expressed in observations coincide with trading days. The sensitivity of the results to the calendar alignment, to the choice of data vendor, to the return frequency, to extreme observations, to the volatility measure and to the sample period is examined explicitly in the robustness section.

Daily percentage logarithmic returns are computed as in Equation (1),

$$r_{i,t} = 100\big(\ln P_{i,t} - \ln P_{i,t-1}\big), \quad i = 1, \dots, N \qquad (1)$$

where $\boldsymbol{P_{i,t}}$ denotes the closing price of asset $\boldsymbol{i}$ on day $\boldsymbol{t}$ and $\boldsymbol{N = 10}$ is the number of assets in the system.

The variables used in the study, their symbols, definitions and theoretical expectations are summarised in Table 1. The variables comprise price and return series (Sayed & Auret, 2019), conditional volatility processes (Clewlow et al., 2014), connectedness measures (Ren et al., 2025; Wang et al., 2026), block spillover indicators (Abdullah et al., 2026) and dynamic correlation measures (Demiralay et al., 2019).

Table 1.

Variables Used in the Study, Their Definitions and Expected Signs/Hypotheses

Variable (symbol)	Definition and description	Expected sign / hypothesis	Source
Price, $P_{i,t}$	Daily US dollar closing price of asset i; futures contract for commodities, spot price for cryptocurrencies.	$I(1)$ in levels; contains a unit root.	Nakajima (2020)
Logarithmic return, $r_{i,t} = 100\,\Delta\ln P_{i,t}$	Daily continuously compounded percentage return; input to the conditional volatility model.	Stationary ($I(0)$); volatility clustering and fat tails expected.	Sayed and Auret (2019); van Oordt et al. (2021)
Conditional volatility, $\sigma_{i,t}$	Time-varying standard deviation estimated by GARCH(1.1); the variable entering the connectedness system.	Positive; high persistence ($\alpha_i + \beta_i$ close to unity); higher levels for cryptocurrencies.	Clewlow et al. (2014); Solibakke (2015)
Forecast error variance share, $\theta_{ij}(H)$	Share of asset j's shocks in the H-step forecast error variance of asset i.	Diagonal ($i = j$) dominant; off-diagonal shares larger within blocks than across blocks.	Ren et al. (2025)
Total connectedness, $C(H)$	System average of off-diagonal shares; degree of integration of the system.	$0 < C < 100$; a moderate level (20–40%) expected.	Wang et al. (2026)
Transmission, TO_i	Connectedness transmitted by asset i to all other assets.	Large for highly volatile, information-intensive markets.	Ren et al. (2025)
Reception, $FROM_i$	Connectedness received by asset i from all other assets.	Large for safe-haven assets.	Jensen et al. (2018); Niu et al. (2024)
Net connectedness, $NET_i = TO_i - FROM_i$	Net balance of directional spillovers.	$NET > 0$ net transmitter; $NET < 0$ net receiver.	Li et al. (2026)
Block connectedness, B_{GH}	Total share transmitted from block G to block H (commodity/crypto blocks).	**Main hypothesis:** within-block $\gg$ cross-block; cross spillover negligible.	Abdullah et al. (2026); Korolev (2026)
Dynamic connectedness, $C_t(H)$	Time-varying total connectedness computed over 250-day rolling windows.	Time-varying; rises during crisis periods.	Page and Panariello (2018); Zainudin and Mohamad (2023)
Conditional correlation, $\rho_{ij,t}$	Time-varying pairwise correlation obtained from the DCC model.	Low for commodity–crypto pairs (≈ 0.1); high for within-block pairs.	Demiralay et al. (2019); Rezitis et al. (2024)
Standardised residual, $z_{i,t} = \varepsilon_{i,t}/\sigma_{i,t}$	Scaled residual used in model diagnostics and in the second step of DCC.	Should be free of autocorrelation and ARCH effects.	Solibakke (2015)

Note: Δ denotes the first-difference operator; H the forecast horizon; and $\mathrm{G}, \mathrm{H} \in \{\text{commodity, crypto}\}$ the block sets. All prices are in US dollars. The "expected sign / hypothesis" column summarises theoretical priors; the empirical tests are presented in the results and robustness sections.

Conditional volatility model

The conditional volatility that serves as the input to the connectedness analysis is obtained from a GARCH(1.1) model (Engle, 1982) estimated separately for each series.

In the constant-mean specification, with $r_{i,t} = \mu_i + \varepsilon_{i,t}$ and $\varepsilon_{i,t} = \sigma_{i,t} z_{i,t}$, the conditional variance is defined as in Equation (2),

$$\sigma_{i,t}^2 = \omega_i + \alpha_i \, \varepsilon_{i,t-1}^2 + \beta_i \, \sigma_{i,t-1}^2 \tag{2}$$

where $\boldsymbol{\omega_i > 0}$, $\boldsymbol{\alpha_i, \beta_i \geq 0}$, and $\boldsymbol{\alpha_i + \beta_i < 1}$ is the stationarity condition. The sum $\boldsymbol{\alpha_i + \beta_i}$ measures volatility persistence. The resulting $\boldsymbol{\sigma_{i,t}}$ series constitute the variables of the connectedness system. The adequacy of the specification is further examined against a Student-t error distribution alternative (Bollerslev, 1987) and through Ljung–Box and ARCH-LM diagnostics (Engle, 1982; Ljung & Box, 1978) on the standardized residuals (see the diagnostics subsection below).

The Diebold–Yılmaz connectedness framework

A VAR model with p lags is fitted to the conditional volatility series $\boldsymbol{x}_t = (\sigma_{1,t}, \ldots, \sigma_{N,t})'$ (Equation 3):

$$\boldsymbol{x}_t = \sum_{i=1}^{p} \boldsymbol{\Phi}_i \, \boldsymbol{x}_{t-i} + \boldsymbol{\varepsilon}_t, \qquad \boldsymbol{\varepsilon}_t \sim (\boldsymbol{0}, \boldsymbol{\Sigma}) \tag{3}$$

Under the stationarity condition, the infinite moving average representation of the system (Equation 4)

$$\boldsymbol{x}_t = \sum_{h=0}^{\infty} \boldsymbol{A}_h \, \boldsymbol{\varepsilon}_{t-h} \tag{4}$$

is obtained, where the coefficient matrices A_h are computed through the recursion $A_h = \Phi_1 A_{h-1} + \cdots + \Phi_p A_{h-p}$ with the initial condition $A_0 = I_N$.

Instead of the Cholesky decomposition, which is sensitive to variable ordering, the ordering-invariant generalized forecast error variance decomposition (GFEVD) of Koop et al. (1996) and Pesaran and Shin (1998) is employed. The contribution of the shocks of variable j to the H-step forecast error variance of variable i is defined as in Equation (5),

$$\theta_{ij}(H) = \frac{\sigma_{jj}^{-1} \sum_{h=0}^{H-1} \left(\boldsymbol{e}_i' \boldsymbol{A}_h \boldsymbol{\Sigma} \boldsymbol{e}_j \right)^2}{\sum_{h=0}^{H-1} \boldsymbol{e}_i' \boldsymbol{A}_h \boldsymbol{\Sigma} \boldsymbol{A}_h' \boldsymbol{e}_i} \tag{5}$$

where $\boldsymbol{\Sigma}$ is the residual covariance matrix, σ_{jj} its j-th diagonal element, and $\boldsymbol{e}_i$ the selection vector whose i-th element equals one and all others zero. Because row sums do not equal one in the generalized decomposition, the shares are normalized row by row (Equation 6):

$$\tilde{\theta}_{ij}(H) = \frac{\theta_{ij}(H)}{\sum_{k=1}^{N} \theta_{ik}(H)}, \qquad \sum_{j=1}^{N} \tilde{\theta}_{ij}(H) = 1 \tag{6}$$

Total connectedness is the system average of the off-diagonal shares (Equation 7):

$$C(H) = \frac{100}{N} \sum_{\substack{i,j=1 \\ i \neq j}}^{N} \tilde{\theta}_{ij}(H) \tag{7}$$

The directional connectedness measures give the shares that asset i receives from the others (Equation 8) and transmits to the others (Equation 9):

$$FROM_i(H) = \frac{100}{N} \sum_{\substack{j=1 \\ j \neq i}}^{N} \tilde{\theta}_{ij}(H), \tag{8}$$

$$TO_i(H) = \frac{100}{N} \sum_{\substack{j=1 \\ j \neq i}}^{N} \tilde{\theta}_{ji}(H) \tag{9}$$

The difference between the two defines net connectedness (Equation 10):

$$NET_i(H) = TO_i(H) - FROM_i(H) \tag{10}$$

Assets with $NET_i > 0$ are net transmitters of volatility to the system, while those with $NET_i < 0$ are net receivers. The net pairwise connectedness between two assets is computed as in Equation (11):

$$NPD_{ij}(H) = \frac{100}{N} \left(\tilde{\theta}_{ji}(H) - \tilde{\theta}_{ij}(H) \right) \tag{11}$$

The lag length p was selected by the Akaike information criterion (AIC; Akaike, 1974) in the level VAR, and the forecast horizon was set to $H = 10$ days. The effect of both choices on the results is examined in the robustness analyses. Horizons and window lengths are counted in observations of the common calendar rather than in calendar days.

Block (group) connectedness

The central contribution of the study is the decomposition of total connectedness at the block level. Summing the entries of the variance decomposition matrix over groups of assets follows from its network interpretation (Diebold & Yilmaz, 2014); the contribution here lies in applying this aggregation to the commodity–cryptocurrency margin and in reporting the four components exactly. The asset set is partitioned into two disjoint blocks: the commodity block $\mathcal{C}$ (six futures contracts) and the crypto block $\mathcal{K}$ (four cryptocurrencies). The connectedness transmitted from block G to block H is defined as in Equation (12):

$$B_{G \to H}(H) = \frac{100}{N} \sum_{i \in H} \sum_{\substack{j \in G \\ j \neq i}} \tilde{\theta}_{ij}(H) \tag{12}$$

By construction, the four block components $\boldsymbol{B_{\mathcal{C} \to \mathcal{C}}}$, $\boldsymbol{B_{\mathcal{K} \to \mathcal{C}}}$, $\boldsymbol{B_{\mathcal{C} \to \mathcal{K}}}$ and $\boldsymbol{B_{\mathcal{K} \to \mathcal{K}}}$ sum to the total connectedness $\boldsymbol{C(H)}$; total connectedness is thus decomposed exactly

into its within-block and cross-block components. The main hypothesis of the study is that the within-block components dominate the cross-block components, and hence that the two markets remain segmented in terms of volatility.

Dynamic (rolling window) connectedness

The evolution of connectedness over time is tracked with rolling windows of $\boldsymbol{W = 250}$ observations of the common calendar (approximately one trading year). At each point $\boldsymbol{t}$, Equations (3), (7) are re-estimated using the observations in the interval $[\boldsymbol{t - W + 1, t}]$, yielding $\boldsymbol{C_t(H)}$. To limit the computational burden, the window is advanced in five-observation steps, and the VAR lag length is capped at two in the short windows. The effect of the window width on the results is examined with four alternative widths in the robustness analyses.

DCC-GARCH dynamic correlation

As complementary evidence at the level of return co-movement, dynamic conditional correlations (Engle, 2002) are estimated for selected pairs. In the first step of the two-step approach, Equation (2) is estimated for each series and the standardised residuals $z_{i,t} = \varepsilon_{i,t}/\sigma_{i,t}$ are obtained. In the second step, the DCC (1.1) dynamics are specified as in Equation (13),

$$\boldsymbol{Q}_t = (1 - a - b)\,\bar{\boldsymbol{Q}} + a\,\boldsymbol{z}_{t-1}\boldsymbol{z}'_{t-1} + b\,\boldsymbol{Q}_{t-1} \qquad (13)$$

where $\bar{\boldsymbol{Q}}$ is the unconditional covariance matrix of the standardised residuals, and $a, b \geq 0$ with $a + b < 1$ as the stationarity condition. The conditional correlation matrix is normalised as in Equation (14),

$$\boldsymbol{R}_t = \mathrm{diag}(\boldsymbol{Q}_t)^{-1/2}\,\boldsymbol{Q}_t\,\mathrm{diag}(\boldsymbol{Q}_t)^{-1/2} \qquad (14)$$

and the pairwise conditional correlation is obtained as in Equation (15):

$$\rho_{ij,t} = \frac{q_{ij,t}}{\sqrt{q_{ii,t}\,q_{jj,t}}} \qquad (15)$$

The parameters $(\boldsymbol{a}, \boldsymbol{b})$ are estimated by likelihood maximisation; the Nelder–Mead search is started from five different initial values and the solution with the highest likelihood is retained, so that local (boundary) optima are avoided. The pairs were chosen so as to allow both cross-block (commodity–crypto) and within-block (gold–silver, Bitcoin–Ethereum) comparisons.

Results

Descriptive statistics

Table 2 presents the descriptive statistics of the daily percentage returns of the ten assets. Mean daily returns are positive for all assets, but markedly higher for the cryptocurrencies (0.097–0.208) than for the commodities (0.006–0.047). The two blocks are also clearly separated in terms of volatility: the daily standard deviation of the cryptocurrencies ranges from 4.24 to 7.17, whereas for the commodities it lies between 1.06 (gold) and 4.15 (natural gas). That natural gas is by far the most volatile series within the commodity block is consistent with the storage constraints and seasonal demand shocks characteristic of this product.

All series display pronounced excess kurtosis, and the Jarque–Bera test (Jarque & Bera, 1987) rejects normality at the 1% level without exception. Kurtosis reaches an extreme value for WTI crude oil (102.78). The series used here is the continuous nearest-contract series and therefore does not contain the negative settlement price of the expiring May 2020 contract; the extreme values are produced by the collapse of the nearest contract in late April 2020 (−56.86%) and by its reversal as the series rolls to the following contract (+58.12%). The high kurtosis of copper (32.86) and its large negative skewness (−1.67) are consistent with the tariff-driven price collapse of 2025, while the high positive skewness of XRP (1.62) and its maximum return of +74.07% accord with the episodic jump behavior of crypto markets. These findings show that fat tails are present in both blocks and justify GARCH-type modelling (van Oordt et al., 2021).

Table 2.

Descriptive Statistics of Daily Percentage Returns

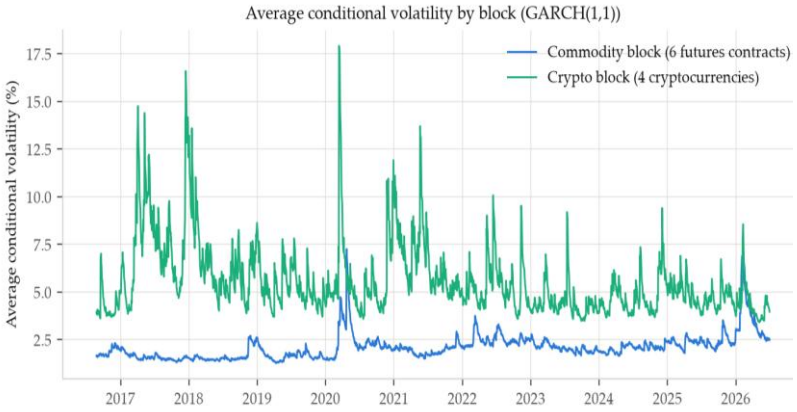
Asset	Mean	Stddev	Skew.	Kurt.	Min.	Max.	JB
Gold	0.045	1.06	-0.76	11.96	-11.41	5.89	8,500
Silver	0.047	2.22	-2.26	40.29	-37.61	13.12	145,297
Copper	0.045	1.55	-1.67	32.86	-24.91	12.33	92,948
Crude Oil	0.017	3.13	-0.50	102.78	-56.86	58.12	1,025,062
Natural Gas	0.006	4.15	-1.19	32.78	-64.40	35.57	91,864
Wheat	0.015	1.99	0.59	8.60	-11.30	19.70	3,370
Bitcoin	0.187	4.24	-0.72	14.36	-49.73	22.76	13,498
Ethereum	0.201	5.82	-0.10	12.38	-58.96	39.25	9,057
XRP	0.208	7.17	1.62	21.73	-54.10	74.07	37,216
Litecoin	0.097	6.17	0.63	15.71	-48.67	60.70	16,808

Note: The sample covers 2,471 common trading days from 25 August 2016 to 30 June 2026. All Jarque–Bera statistics are significant at the 1% level (***p* < .001**). Column labels: Std.dev. = standard deviation, Skew. = skewness, Kurt. = kurtosis, Min./Max. = minimum/maximum, JB = Jarque–Bera statistic.

Return correlations provide a first indication of the block structure. The average within-block correlation is 0.162 for the commodities and 0.598 for the cryptocurrencies, whereas the average cross-block correlation is only 0.058. At the pairwise level, the gold–silver correlation is 0.773 and the Bitcoin–Ethereum correlation 0.716, while gold–Bitcoin remains at 0.092 and crude oil–Bitcoin at 0.051. Figure 1 compares the average conditional volatility paths of the two blocks; the crypto block is systematically more volatile in level, yet the timing of fluctuations in the two series evolves largely independently.

Figure 1.

Average Conditional Volatility of the Commodity and Crypto Blocks (2016–2026).



Stationarity

A precondition of the connectedness analysis is that the variables entering the VAR system be stationary. Table 3 reports unit root test results for both the return and the conditional volatility series (Dickey & Fuller, 1979; Kwiatkowski et al., 1992; Phillips & Perron, 1988). For the return series, the ADF and Phillips–Perron tests strongly reject the null hypothesis of a unit root for all series at the 1% level, while the KPSS test does not reject the null of stationarity for any series. All return series are therefore $\boldsymbol{I(0)}$.

For the conditional volatility series, the ADF and PP tests again reject the unit root for all series (statistics between −3.67 and −9.69). The KPSS statistics, however, exceed the critical values for eight of the ten series, rejecting stationarity; only for crude oil (0.178) and wheat (0.430) can stationarity not be rejected. This is a natural consequence of the near-unit persistence of the volatility series (see the diagnostics subsection): the KPSS test is known to over-reject in finite samples for highly persistent yet stationary processes. In this situation of conflicting verdicts between the two test families, the joint verdict of the ADF and PP tests, together with the fact that the GARCH estimates satisfy the stationarity constraint ($\boldsymbol{\alpha_i + \beta_i < 1}$), was taken as decisive, and the VAR system was specified on the volatility levels. The impact of this choice on the results is indirectly examined through the lag-length sensitivity analysis (see the robustness analyses).

Table 3.

Unit Root Tests (Test Statistics)

Series	ADF (r)	PP (r)	KPSS (r)	ADF (σ)	PP (σ)	KPSS (σ)
Gold	-20.68	-51.18	0.267	-4.39	-4.37	2.222
Silver	-8.82	-52.72	0.176	-3.78	-3.67	1.724
Copper	-51.96	-52.25	0.044	-4.87	-4.70	2.563
Crude Oil	-9.88	-56.15	0.035	-5.09	-6.32	0.178
Natural Gas	-25.32	-52.86	0.034	-5.07	-5.13	3.119
Wheat	-26.73	-48.33	0.074	-7.41	-6.77	0.430
Bitcoin	-27.05	-51.78	0.340	-9.46	-9.22	1.785
Ethereum	-12.23	-51.54	0.396	-7.65	-7.24	2.163
XRP	-10.39	-49.38	0.211	-5.59	-9.69	1.166
Litecoin	-13.83	-50.05	0.358	-7.59	-7.15	1.550

Note: The null hypothesis is the presence of a unit root for ADF and PP, and stationarity for KPSS. A constant-only specification is used. All ADF and PP statistics are significant at the 1% level. The 5% critical value for KPSS is 0.463. Column labels: r = return series, σ = conditional volatility series.

Static connectedness and directional spillovers

Table 4 reports the directional and net volatility connectedness of the ten-asset system. The lag length selected by the AIC is four and the forecast horizon is ten days. Total connectedness in the system is 28.7%; that is, roughly 29% of the ten-day forecast error variance of the average asset stems from the shocks of the other assets, while 71% stems from its own shocks. This value indicates that the system is not entirely independent, but neither is it highly integrated.

Natural gas (+20.4) leads the ranking of net transmitters by a wide margin, followed by Ethereum (+8.5), Bitcoin (+4.3), Litecoin (+3.4) and wheat (+0.5). The net receivers are gold (−18.7), XRP (−14.2), copper (−2.6), crude oil (−1.2) and silver (−0.4). Gold's position as the largest net receiver is striking: gold receives markedly more from the system (46.7) than it transmits to it (28.0). This finding can be interpreted consistently with gold's safe-haven character; rather than generating shocks of its own, gold acts as an asset that absorbs uncertainty originating in other markets

(Jensen et al., 2018; Niu et al., 2024).

That the cryptocurrencies exhibit high values on both the transmission and the reception side (Ethereum 57.7/49.2; Bitcoin 52.6/48.3) might at first sight suggest that these assets interact intensively with the system as a whole. As the block decomposition below will show, however, this interaction takes place almost entirely within the crypto block. This is an important caution against interpreting total and directional measures in isolation.

Table 4.
Directional and Net Volatility Connectedness (%)

Asset	Transmission (TO)	Reception (FROM)	Net
Natural Gas	22.5	2.1	+20.4
Ethereum	57.7	49.2	+8.5
Bitcoin	52.6	48.3	+4.3
Litecoin	48.0	44.6	+3.4
Wheat	1.6	1.0	+0.5
Silver	41.0	41.4	-0.4
Crude Oil	5.1	6.3	-1.2
Copper	6.3	8.9	-2.6
XRP	24.3	38.5	-14.2
Gold	28.0	46.7	-18.7
Total connectedness			**28.7**

Note: Net = TO − FROM. A positive net value indicates a net transmitter, a negative net value a net receiver. The VAR lag length was set to four by the AIC and the forecast horizon to ten days.

Block spillovers: segmentation between commodities and crypto

The central finding of the study emerges from the block-level decomposition of total connectedness (Table 5). The components of total connectedness (28.7%) are as follows: spillover within the commodity block 10.03 points, spillover within the crypto block 17.63 points, spillover from the crypto block to the commodity block 0.62 points, and spillover from the commodity block to the crypto block only 0.42 points.

This decomposition shows that 61.4% of total connectedness occurs within the crypto block and 34.9% within the commodity block, while cross-block transmission accounts for only 3.6% of the total. In other words, more than nineteen twentieths of the volatility interaction measured in the system remains within the blocks. This finding gives concrete form to the interpretive pitfall noted above: Bitcoin's high transmission value of 52.6% does not mean that this asset exports volatility to commodity markets; almost all of that transmission is directed at the other cryptocurrencies.

The heat map of the generalized forecast error variance decomposition in Figure 2 confirms this structure visually: the high-spillover cells cluster in the crypto–crypto and precious metal–precious metal corners, while the commodity–crypto cross cells are almost empty. Figure 3 compares the shares of the block components in the total, and Figure 4 displays the ranking of net transmitters and receivers.

This finding is also consistent with the return correlations reported above: the average within-block correlations (commodities 0.162; crypto 0.598) lie well above the cross-block correlation (0.058). The two markets are therefore segmented at the level of both the first moment (returns) and the second moment (volatility).

Table 5.
Block Connectedness Matrix (%)

Receiver Transmitter	Commodity block	Crypto block	Total (FROM)
Commodity block	10.03	0.62	10.65
Crypto block	0.42	17.63	18.05
Total (TO)	10.45	18.26	28.71

Note: The cells are the sums of the normalised shares divided by system size, as defined in Equation (12); the four components sum exactly to total connectedness (28.7%). Rows denote the receiving (FROM) block, columns the transmitting (TO) block. Block shares: within-commodity 34.9%, within-crypto 61.4%, cross-block 3.6%.

Figure 2.
Heat Map of the Generalized Forecast Error Variance Decomposition (%).

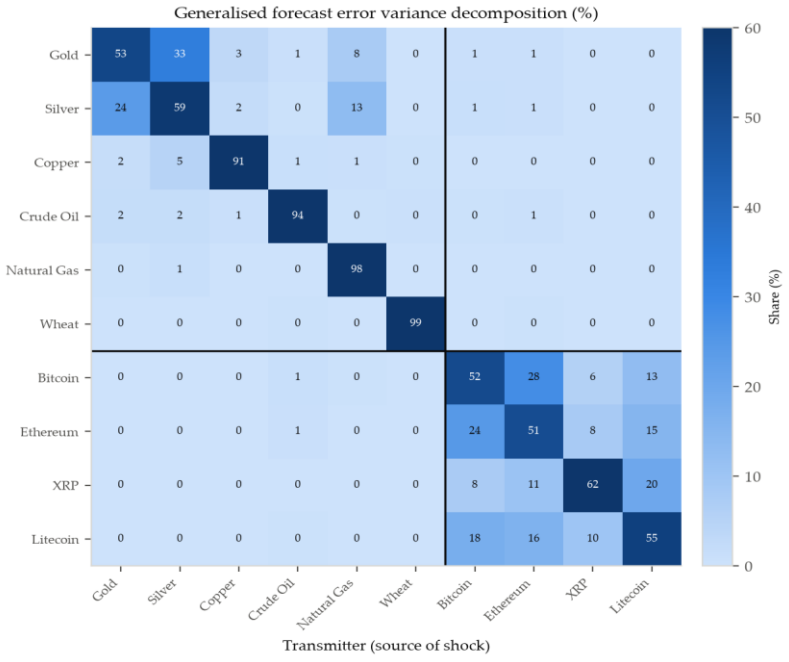


Figure 3.
Decomposition of Total Connectedness Into Block Components.

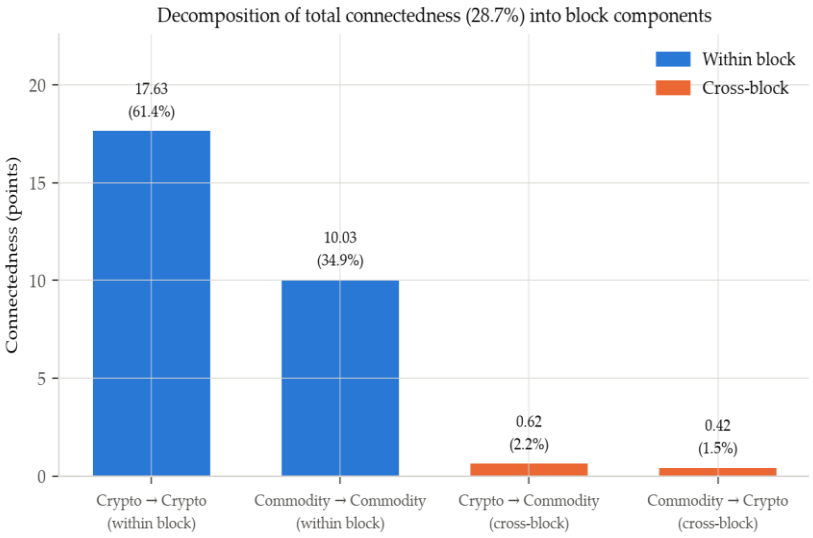
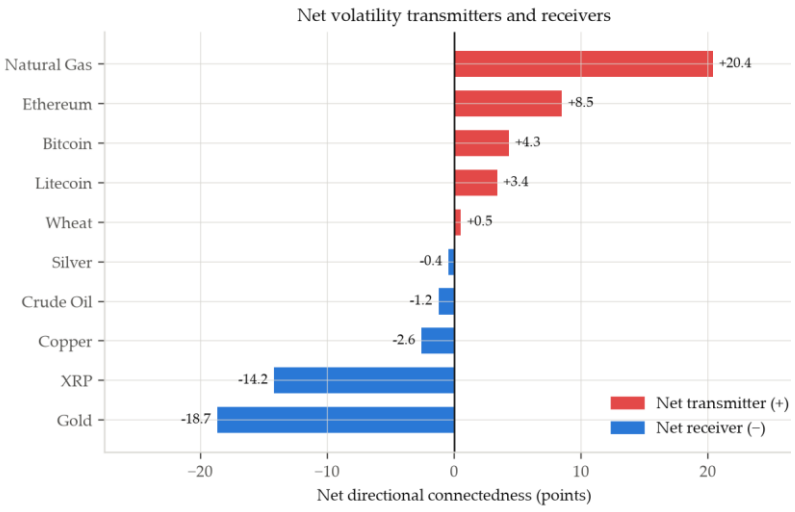


Figure 4.
Net Volatility Transmitters and Receivers.



Net pairwise connectedness

The block structure is also evident at the pairwise level (Table 6). All eight of the largest net pairwise connectedness values in absolute terms occur in within-block pairs: from natural gas to silver (+1.180) and to gold (+0.746), from silver to gold (+0.914) and from copper to silver (−0.287) within the commodity block, and from Litecoin to XRP (+0.983) and to Bitcoin (−0.511), from Ethereum to Bitcoin (+0.362) and from XRP to Ethereum (−0.269) within the crypto block. The transmissions from natural gas reflect its position as the dominant net transmitter within the commodity block. Not a single commodity–crypto pair appears among the eight largest net pairwise linkages. This table shows that segmentation is not an averaging artefact at the aggregate level; it holds systematically at the level of pairwise relations as well.

Table 6.
Largest Net Pairwise Connectedness Values

Source (net transmitter)	Target (net receiver)	Net pairwise
Natural Gas	Silver	+1.180
Litecoin	XRP	+0.983
Silver	Gold	+0.914
Natural Gas	Gold	+0.746
Litecoin	Bitcoin	-0.511
Ethereum	Bitcoin	+0.362
Copper	Silver	-0.287
XRP	Ethereum	-0.269

Note: Net pairwise connectedness is computed from Equation (11). A negative value indicates that the transmission runs in the direction opposite to the one stated. The eight largest pairs in absolute value are reported.

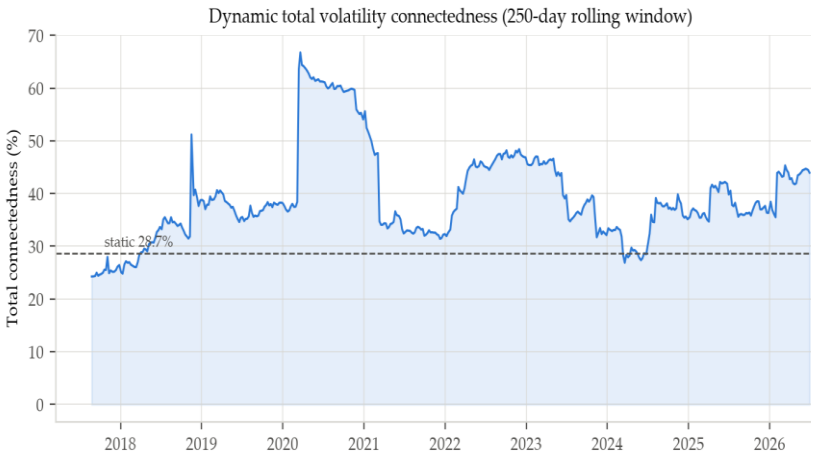
Dynamic connectedness

Total connectedness is not constant over time. Dynamic total connectedness computed with a 250-day rolling window averages 39.3%, fluctuating between 24.3% and 66.8% (Figure 5). That dynamic average exceeds the static value (28.7%) is not a contradiction but a methodological consequence: because short windows rely on fewer observations and a more restricted lag structure, estimated connectedness is systematically biased upwards. Indeed, as shown below, the dynamic average declines and approaches the static value as the window widens.

The timing of connectedness is economically meaningful. In the first half of 2020, when the COVID-19 pandemic hit global markets, dynamic connectedness rose to an average of 56.7%; throughout 2022 (the period of the energy shock and monetary tightening) it hovered around 45.1%; and in 2025 it receded to 37.8%. This pronounced rise during crises is consistent with the established finding that cross-asset linkages tighten under stress (Page & Panariello, 2018; Zainudin & Mohamad, 2023) and is critical from a diversification standpoint: even though block segmentation is strong on average, the system as a whole becomes temporarily more integrated during crisis periods.

Figure 5.

Dynamic Total Volatility Connectedness (250-Day Rolling Window).



Pairwise dynamic correlations

Block segmentation is also supported by DCC-GARCH, which operates on return shocks rather than on conditional volatilities (Table 7). The conditional correlations of the commodity–crypto pairs are low and positive, averaging between 0.040 and 0.123. The highest average correlations arise for the silver–Bitcoin (0.123) and copper–Bitcoin (0.099) pairs, and the lowest for crude oil–Bitcoin (0.040). Although the correlations occasionally approach zero, they rarely turn negative (the share of time spent in negative territory is at most 7.8%).

For the within-block pairs, by contrast, the picture changes entirely: the Bitcoin–Ethereum conditional correlation averages 0.758 and gold–silver 0.784. Within-block correlations are thus roughly nine times the cross-block correlations on average, and at least six times the largest of them. Figure 6 plots the evolution of the commodity–Bitcoin conditional correlations, and Figure 7 compares the within-block and cross-block correlations; the bands of the two groups do not overlap in any period.

The DCC parameters support this segmentation as well. In the within-block pairs the correlation dynamics are lively (Bitcoin–Ethereum $\boldsymbol{a = 0.054}$, $\boldsymbol{b = 0.940}$; gold–silver $\boldsymbol{a = 0.025}$, $\boldsymbol{b = 0.962}$) and the correlation varies substantially over time for Bitcoin–Ethereum (standard deviation 0.192), while the gold–silver correlation is high but comparatively stable (0.047). In the commodity–crypto pairs, the $\boldsymbol{a}$ parameter takes very small values of 0.001–0.009 and correlation volatility remains low (0.009–0.060). This shows that cross-block correlations are not merely low but also inert unresponsive to new information.

Because the likelihood is maximised from five different starting values, none of the seven pairs converged to a boundary (degenerate) solution: the estimated parameters lie strictly inside the admissible region for every pair and the persistence a + b ranges from 0.973 to 0.997. The commodity–crypto pairs nevertheless differ from the within-block pairs in kind and not only in level: their news-impact parameter is an order of magnitude smaller, so that their conditional correlations move slowly and within a narrow band.

Table 7.

Dynamic Conditional Correlations (DCC-GARCH)

Statistic	P1	P2	P3	P4	P5	P6	P7
Uncond. corr.	0.092	0.083	0.100	0.051	0.117	0.716	0.773
DCC mean	0.094	0.089	0.099	0.040	0.123	0.758	0.784
DCC std. dev.	0.053	0.009	0.034	0.030	0.060	0.192	0.047
Minimum	-0.057	0.063	0.029	-0.043	-0.027	-0.035	0.594
Maximum	0.263	0.115	0.172	0.183	0.303	0.970	0.887
Negative time (%)	3.7	0.0	0.0	7.8	0.6	0.3	0.0
a	0.008	0.001	0.003	0.006	0.009	0.054	0.025
b	0.980	0.986	0.993	0.967	0.979	0.940	0.962

Note: Obtained from two-step DCC(1.1) estimation. P6 and P7 are the within-block (comparison) pairs. "Negative time" is the share of observations in which the correlation is negative. Pairs: P1 = Gold–Bitcoin, P2 = Gold–Ethereum, P3 = Copper–Bitcoin, P4 = Crude Oil–Bitcoin, P5 = Silver–Bitcoin, P6 = Bitcoin–Ethereum, P7 = Gold–Silver. Row labels: Uncond. = unconditional correlation; Neg. time = share of observations with a negative correlation.

Figure 6.

Dynamic Conditional Correlation Between Commodities and Bitcoin.

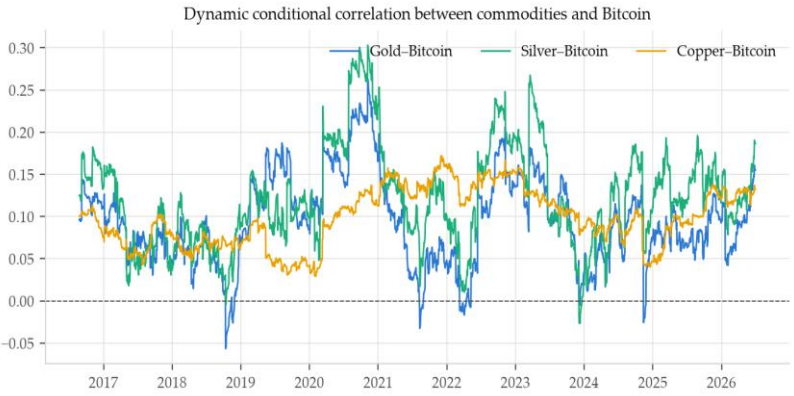
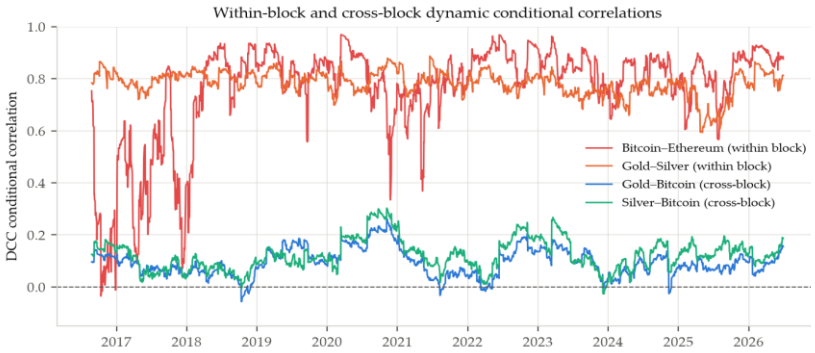


Figure 7.

Comparison of Within-Block and Cross-Block Dynamic Conditional Correlations.



Robustness and Diagnostic Analyses

This section examines the resilience of the main findings to model specification and methodological choices from four angles: (i) specification diagnostics of the conditional volatility model, (ii) sensitivity to the forecast horizon and the VAR lag length, (iii) sensitivity to the rolling window width, and (iv) sensitivity to the data source and calendar alignment, the return frequency, extreme observations, the volatility measure and the sample period.

Diagnostics of the conditional volatility model

Table 8 presents a comparison of the GARCH specifications feeding the connectedness system, along with diagnostics on the standardized residuals. The Student-t error distribution lowers the AIC relative to the normal distribution for all ten series; the gain is especially large for the cryptocurrencies (for XRP, for instance, from 15,964 to 15,000). The degrees-of-freedom parameter $\boldsymbol{\nu}$ takes extremely low values of 2.82–3.18 for the cryptocurrencies; this points to tails so heavy that even the fourth moment (kurtosis) may be undefined, and it is consistent with the excess kurtosis findings in Table 2. For the commodities, $\boldsymbol{\nu}$ lies in the range 3.79–9.27.

Volatility persistence ($\boldsymbol{\alpha} + \boldsymbol{\beta}$) is very close to unity for nine of the ten series (0.953–1.000), the single exception being copper (0.900). For three of the four cryptocurrencies (Bitcoin, XRP and Litecoin) persistence is estimated at 1.000 to three decimal places, and for Ethereum at 0.991; this points to integrated-GARCH (IGARCH) type behaviour, in which the effect of shocks on the conditional variance effectively fails to die out. While this finding shows that crypto volatility displays a persistent and predictable clustering structure, persistence so close to the unit value means that the estimation operates at the boundary of the stationarity constraint, which should be recorded as a limitation.

Table 8.

GARCH(1.1) Specification Comparison and Residual Diagnostics

Series	α+β	ν	AIC (N)	AIC (t)	LB(10) p	ARCH(10) p
Gold	0.995	4.15	6,830	6,578	0.756	0.046
Silver	0.997	3.79	10,020	9,697	0.296	0.422
Copper	0.900	5.16	8,931	8,662	0.701	1.000
Crude Oil	0.961	5.50	11,017	10,812	0.827	0.001
Natural Gas	0.997	5.32	13,205	12,956	0.101	0.079
Wheat	0.953	9.27	10,074	10,032	0.079	0.276
Bitcoin	1.000	3.18	13,803	13,269	0.043	0.021
Ethereum	0.991	3.09	15,325	14,869	0.016	0.175
XRP	1.000	2.82	15,964	15,000	0.303	0.997
Litecoin	1.000	3.00	15,625	14,926	0.550	0.999

Note: The α+β and ν values are from the GARCH(1.1)-t estimation. The Ljung–Box and ARCH-LM tests are applied to the standardised residuals (z) and their squares (z^2) with ten lags. A high p-value indicates that the null hypothesis (no autocorrelation / no ARCH effects) cannot be rejected. Column labels: AIC (N) = AIC under the normal distribution, AIC (t) = AIC under the Student-t distribution, LB = Ljung–Box, ARCH = ARCH-LM.

Sensitivity to the forecast horizon and lag length

The connectedness measures depend on two methodological choices: the forecast horizon $\boldsymbol{H}$ and the VAR lag length $\boldsymbol{p}$. Table 9 examines the impact of these choices. When the forecast horizon is reduced to five days, total connectedness moves to 26.3%; when it is extended to twenty days, it moves to 31.8%. This reflects the additional time allowed for shocks to propagate at longer horizons; the range is nevertheless narrow and leaves the qualitative conclusion unchanged.

The lag-length sensitivity is more critical for the main finding of the study. As the lag is raised from one to six, total connectedness increases from 26.2% to 29.1%. Over the same range, spillover from commodities to crypto varies between 0.14 and 0.58 points, and spillover from crypto to commodities between 0.55 and 0.95 points. Even under the most generous specification (p = 6), therefore, total cross-block spillover remains at 1.53 points corresponding to only 5.3% of total connectedness under that specification (29.1%). The commodity–crypto segmentation is thus robust to the lag choice and is not an artefact of the baseline specification.

Table 9.

Robustness: Sensitivity to the Forecast Horizon and VAR Lag Length (%)

Specification	Total	Comm.→Crypto	Crypto→Comm.
Horizon H=5	26.33	—	—
Horizon H=10 (baseline)	28.71	—	—
Horizon H=20	31.81	—	—
Lag p=1	26.19	0.14	0.55
Lag p=2	27.71	0.21	0.66
Lag p=4 (baseline, AIC)	28.71	0.42	0.62
Lag p=6	29.07	0.58	0.95

Note: In the horizon rows the lag length is set by the AIC (four); in the lag rows the forecast horizon is fixed at ten days. The baseline specification is marked. 'Total' is total connectedness; Comm. = commodity block, Crypto = crypto block.

Sensitivity to the rolling window width

The dynamic connectedness results depend on the choice of rolling window width. Table 10 compares the results across four alternative widths (150, 200, 250 and 300 days). As the window widens, average connectedness declines systematically: 45.8% at 150 days, 41.8% at 200 days, 39.3% at 250 days and 37.6% at 300 days. This pattern directly supports the explanation advanced above that short windows generate an upward bias and identifies the methodological source of the dynamic average exceeding the static value (28.7%).

What matters is that the qualitative conclusion is preserved across all windows: connectedness is markedly time-varying at every width (even at 300 days, the narrowest range is 23.1–63.1%) and rises during crisis periods. The level of dynamic connectedness is therefore sensitive to the window choice, but its pattern over time is not.

Table 10.

Robustness: Sensitivity to the Rolling Window Width (%)

Window (days)	Mean	Minimum	Maximum
150	45.8	27.6	73.1
200	41.8	24.9	67.9
250 (baseline)	39.3	24.3	66.8
300	37.6	23.1	63.1

Note: In all windows the forecast horizon is ten days and the VAR lag length is capped at two. The window is advanced in five-day steps.

Sensitivity to the data source, the return frequency, extreme observations and the sample period

The block decomposition rests on a series of construction choices: which vendor supplies the price series, how the series are aligned in calendar time, at what frequency returns are computed, how extreme observations are treated, which statistic represents volatility, and over which period the system is estimated. Table 11 reports the block decomposition under fourteen alternative specifications covering these five dimensions. Total connectedness stays within a narrow band (27.3%–32.6%) in every case except the weekly and subperiod specifications discussed below, and within-block transmission dominates in all of them.

Panel A concerns the data. The gold and silver futures series used here report all five weekdays. An alternative vendor series for the same two contracts omits Friday closes over much of the sample, so that about one quarter of the resulting returns span a Thursday-to-Monday interval; re-estimating the system on that series raises the cross-block share from 3.6% to 9.9%. The source of the difference is silver rather than gold: restoring the complete calendar for silver alone already gives 3.8%, whereas restoring it for gold alone leaves the share at 10.1%. The mechanism is transparent. Multi-period returns aggregate information that would otherwise be distributed over several observations, which mechanically raises contemporaneous co-movement across markets, and in a GARCH setting such observations are read as unusually large shocks. Irregular spacing therefore inflates, rather than deflates, measured cross-block spillover. Replacing gold futures with the spot gold series of the second vendor a different price, a different vendor and a complete calendar gives 4.7%, so the result is not an artefact of the vendor chosen.

Panels B to D vary the construction of the variables. At the weekly frequency the cross-block share rises to 16.0% of a higher total (36.8%). Weekly sampling removes the non-synchronous closing of the two markets (Martens & Poon, 2001) and at the same time reduces the sample to 514 observations, which biases connectedness upwards, so the two effects cannot be separated within this design; a frequency-domain decomposition (Baruník & Křehlík, 2018) would be the natural way to characterise this dimension. Winsorising the commodity returns at the 0.5% and 99.5% quantiles, which removes the roll-date outliers discussed in the data section, gives 4.6%, and scaling each return by the square root of the number of days it spans, in the spirit of the trading-time variance adjustment of French and Roll (1986), gives 3.7%. Replacing the GARCH(1.1) conditional standard deviation by its Student-t counterpart, by its logarithm or by the Parkinson range estimator leaves the cross-block share between 2.0% and 3.9%, which shows that the finding does not depend on the particular volatility proxy entering the VAR.

Panel E divides the sample into four consecutive subperiods of 617 observations each. The cross-block share is 27.9% and 27.3% in the two earliest subperiods, 14.4% in 2021–2024 and 9.7% in the most recent one, while total connectedness itself varies markedly (19.0%–42.4%). Part of this variation is the upward small-sample bias documented in the previous subsection, but the monotone decline of the cross-block share across the four subperiods is informative in its own right: the segmentation of the two markets has become more, not less, pronounced as the crypto market has matured, which is consistent with the institutionalisation of crypto trading documented by Hornback and Whaley (2025). Within-block transmission dominates in every subperiod. The qualitative conclusion is therefore robust along all five dimensions; the specific figure of 3.6% pertains to the daily frequency and to the full sample.

Discussion

The findings consistently indicate that commodity futures markets and cryptocurrency markets form two segmented blocks in terms of volatility. Three lines of evidence point to this conclusion: the block connectedness decomposition (cross-block spillover accounts for only 3.6% of the total), the concentration of the largest net pairwise linkages exclusively in within-block pairs, and DCC conditional correlations for cross-block pairs at roughly one ninth the level of within-block pairs. That all three measures point in the same direction indicates that the finding is not the product of any single measure.

The economic interpretation of this segmentation is that the two markets are driven by different sources of shocks. Commodity volatility is shaped by supply constraints, inventory dynamics, weather conditions, geopolitical developments and macroeconomic news flow (Calomiris et al., 2026; Chen & Yu, 2025; Hess et al., 2008), whereas crypto volatility is moulded by regulatory developments, protocol and infrastructure events, exchange risks and idiosyncratic investor sentiment (Edwards et al., 2019; Yang & Kwon, 2026). The absence of a common systematic factor is meaningful when set against evidence documenting the existence of such a factor among commodities themselves (Etienne et al., 2025): the common factor operates within the block but not across blocks. Korolev's (2026) finding that decentralized finance assets exhibit limited correlation with traditional assets is likewise consistent with this framework.

Table 11.

Robustness: Block Decomposition Under Alternative Data, Frequency, Outlier, Volatility-Measure and Sample-Period Specifications (%)

Specification	Total	Within-block	Cross-block
A. Data source and calendar alignment			
Baseline: complete calendar, daily returns (N = 2,471)	28.71	96.4	3.6
Alternative vendor series, incomplete Friday coverage (N = 1,989)	27.89	90.1	9.9
Spot gold in place of gold futures (N = 2,471)	28.17	95.3	4.7
B. Return frequency			
Weekly returns (N = 514)	36.81	84.0	16.0
C. Extreme observations and interval length			
Commodity returns winsorised at 0.5% / 99.5%	27.27	95.4	4.6
Returns scaled by the square root of the days spanned	30.00	96.3	3.7
D. Volatility measure entering the VAR			
GARCH(1.1)-t conditional standard deviation	29.03	96.1	3.9
Log GARCH(1.1) conditional standard deviation	28.29	98.0	2.0
Parkinson range volatility	32.56	96.2	3.8
Log Parkinson range volatility	29.71	96.8	3.2
E. Sample period (617 observations each)			
August 2016 – February 2019	18.95	72.1	27.9
February 2019 – July 2021	42.42	72.7	27.3
July 2021 –	34.65	85.6	14.4

Specification	Total	Within-block	Cross-block
January 2024			
January 2024 – June 2026	33.92	90.3	9.7

Note: 'Total' is total connectedness. 'Within-block' is the sum of the within-commodity and within-crypto components expressed as a percentage of total connectedness, and 'Cross-block' is the sum of the two cross-block components on the same basis; the two columns sum to 100. Unless stated otherwise the forecast horizon is ten observations, the VAR lag length is selected by the AIC and the sample comprises 2,471 observations. The baseline row reproduces Table 5.

From a methodological standpoint, the study's most important implication is that interpreting the total connectedness measure in isolation can be misleading. The system's total connectedness of 28.7% could, on a superficial reading, be interpreted as "commodity and crypto markets are moderately integrated." The block decomposition shows, however, that almost all of this value stems from within-block interaction. The same fallacy applies to the directional measures: Bitcoin's transmission value of 52.6% reflects not the export of volatility to the broader system but its dominant position within the crypto block. This observation suggests that block-level decomposition should become a standard complementary analysis in connectedness studies built on heterogeneous asset sets.

The dynamic findings, in turn, are a reminder that segmentation is not unconditional. The rise of connectedness to 56.7% during the COVID-19 period shows that the system temporarily becomes more integrated under stress. This accords directly with Page and Panariello's (2018) warning that diversification fails when it is needed most, and it qualifies the study's diversification implication: commodity–crypto diversification is strong on average but weakens somewhat during periods of systemic stress. It should nevertheless be emphasized that even the crisis-period rise falls short of full convergence; even at their highest values (0.263 for gold–Bitcoin), cross-block correlations remain below the average of the within-block correlations (0.76–0.78).

The net spillover pattern likewise displays an economically interpretable structure. Natural gas's dominant net transmitter position within the commodity block is consistent with the storability constraints and seasonal demand shocks of this product, while gold's position as the largest net receiver accords with its safe-haven role. Gold's absorption of external volatility is in line with the literature on this metal's function within portfolios (Jensen et al., 2018; Niu et al., 2024). Within the crypto block, the net transmitter positions of Ethereum and Bitcoin and XRP's net receiver position show that the block possesses an internal hierarchy with the two largest assets at its apex, conceptually parallel to the "core" and "bridge" currencies identified in currency networks (Li et al., 2026).

The robustness analyses reinforce these conclusions: cross-block spillover does not exceed 5.3% of the total under any horizon or lag specification, stays below 5% under every alternative volatility measure, and the time pattern of dynamic connectedness is insensitive to the window width. At the same time, the diagnostics render two limitations visible: the persistence of the crypto series resting on unity and the Student-t degrees of freedom estimated at extremely low values of 2.8–3.2 indicate that risks beyond the second moment (in the tails) may not be fully captured by the standard GARCH framework in these markets. Sharma and Karmakar's (2024) caution that central dependence measures may fail to represent tail behavior is especially pertinent in this context and underscores the complementary value of tail-focused approaches (Abdullah et al., 2026; Ren et al., 2025).

Conclusion and Recommendations

This study has examined the volatility connectedness between six commodity futures contracts and four cryptocurrencies over the period 2016–2026, using 2,471 common daily observations, the Diebold–Yılmaz connectedness framework and the DCC-GARCH model. The main findings are as follows: (i) total volatility connectedness in the system is 28.7%; (ii) 61.4% of this total occurs within the crypto block and 34.9% within the commodity block, leaving cross-block spillover at only 3.6% of the total; (iii) the leading net volatility transmitters are natural gas (+20.4) and Ethereum (+8.5), while the largest net receiver is gold (−18.7); (iv) all eight of the largest net pairwise linkages in absolute value occur in within-block pairs, without a single commodity–crypto pair among them; (v) dynamic connectedness is time-varying (24.3–66.8%) and rises during crises (56.7% during COVID-19); (vi) commodity–crypto pairwise conditional correlations are low and inert (0.040–0.123), whereas within-block correlations are roughly nine times higher (gold–silver 0.784; Bitcoin–Ethereum 0.758).

At the theoretical level, these findings contribute to literature on three points. The first is the demonstration that an exact decomposition of total connectedness into its block components can qualify integration interpretations based on the aggregate measure: connectedness of 28.7% measured in the same system points, when viewed at the block level, not to integration but to segmentation. This suggests that block

decomposition is a valuable complement in connectedness analyses built on heterogeneous asset sets, and it adds to the literature a caution that may be summarized as "total connectedness conceals block structure." Second, the agreement between volatility connectedness and return-level dynamic conditional correlations indicates that the finding is not specific to a single measure. Third, the documentation that cross-block correlations are not only low but also inert (with DCC $\boldsymbol{a}$ parameters taking near-zero values of 0.001–0.009) provides direct evidence that no common dynamic factor responsive to new information links commodity and crypto assets.

For practice and policy, the findings offer implications that differ across stakeholders. For portfolio managers, the low volatility connectedness and the low, stable correlation between commodity and crypto assets indicate that holding the two asset classes together provides strong and relatively durable diversification; however, the rise of dynamic connectedness to as much as 57% during crises carries the warning that this benefit will partially weaken in periods of stress (Page & Panariello, 2018). Moreover, the very high correlation within the crypto block (Bitcoin–Ethereum 0.758) indicates that diversification purely within crypto offers limited benefit, and that crypto assets should be treated largely as a single risk cluster in a portfolio context. For risk managers, the volatility persistence resting on unity estimated for the crypto series and the extremely low degrees of freedom show that value-at-risk calculations for these assets under a normality assumption would be seriously misleading. For regulators and supervisory authorities, the block segmentation can be read in two ways: on the one hand, the risk of shocks in crypto markets spilling over into commodity markets is low (spillover from crypto to commodities is only 0.62 points); on the other hand, this segmentation means that, owing to the high internal connectedness of the crypto markets (17.63 points), systemic risk is concentrated within the block, calling for supervision to be concentrated there as well (Edwards et al., 2019).

Methodologically, the study has combined connectedness measurement with block decomposition, net pairwise analysis and dynamic correlation validation, testing robustness along the dimensions of horizon, lag length, window width, data source, return frequency, outlier treatment, volatility measure and sample period. It nevertheless has certain limitations. First, the two markets do not share a trading calendar: cryptocurrencies trade on weekends while commodity futures do not, so that weekend cryptocurrency movements are absorbed into the first common observation of the following week. The two markets also close at different times of day, which attenuates measured contemporaneous linkages (Martens & Poon, 2001): the average cross-block return correlation is 0.058 at the daily frequency against 0.082 at the weekly frequency, and commodity returns correlate only weakly with lagged cryptocurrency returns (0.018). The net effect of these features is quantified in the robustness section. Second, spot prices were used on the crypto side rather than regulated futures contracts; the futures–spot asymmetry between the commodity and crypto legs is a source of heterogeneity. Third, conditional volatility was measured with univariate GARCH models, and the estimation error that the two-step approach may generate was not accounted for in the second stage. Fourth, the asset cross-section is limited to ten and excludes stablecoins and decentralized finance assets.

Future research can extend this framework in several directions. A frequency-domain connectedness decomposition would separate short- and long-run spillover components and reveal the term structure of block segmentation. Quantile connectedness and tail-focused measures (Abdullah et al., 2026; Ren et al., 2025) could test whether the segmentation observed in average behavior also holds in the extreme tails; the extremely low degrees of freedom reported in the diagnostics make this extension especially necessary. Using regulated crypto futures contracts would remove the spot–futures asymmetry. Furthermore, enlarging the block count with a broader asset cross-section (stablecoins, decentralized finance tokens, tokenized commodities) could establish whether the segmentation is a binary structure or a multi-block hierarchy. Finally, employing realized volatility measures based on high-frequency data would reduce the uncertainty generated by two-step estimation and strengthen the external validity of the findings.

Hakem Değerlendirmesi: Dış bağımsız.
Yazar Katkıları: Bu çalışmanın hem teorik hem de uygulama kısımları tamamen yazar tarafından hazırlanmıştır.
Çıkar Çatışması: Yazar, çıkar çatışması olmadığını beyan etmiştir.
Finansal Destek: Yazar, bu çalışma için finansal destek almadığını beyan etmiştir.
Yapay Zekâ Kullanımı: Bu çalışmada dil kontrolü için yapay zekâ kullanılmıştır. Kullanılan yapay zekâ yazılımları DeepL ve Claude'dur.

Peer-review: Externally peer-reviewed.
Author Contributions: Both the theoretical and practical sections of this study were prepared entirely by the author.
Conflict of Interest: The author has declared that there is no conflict of interest.
Financial Disclosure: The author declared that he received no financial

support for this study.

Use of Artificial Intelligence: Artificial intelligence was used for language editing in this study. The AI software used were DeepL and Claude.

References

Abdullah, M., Tiwari, A. K., Abakah, E. J. A., & Lee, C.-C. (2026). Tail risk connectedness between tokenized and traditional derivatives: Time-frequency analysis and portfolio insights. *Investment Analysts Journal, 55*(2), 195–218. [CrossRef]

Abideen, Z. U., & Wu, K. (2026). Network-based stochastic volatility modeling for interconnected futures markets. *Journal of Futures Markets, 46(9), 1700–1718.* [CrossRef]

Akaike, H. (1974). A new look at the statistical model identification. *IEEE Transactions on Automatic Control, 19*(6), 716–723. [CrossRef]

Albulescu, C. T., Goyeau, D., & Tiwari, A. K. (2017). Co-movements and contagion between international stock index futures markets. *Empirical Economics, 52*(4), 1529–1568. [CrossRef]

Bartolozzi, M., Mellen, C., Di Matteo, T., & Aste, T. (2007). Multi-scale correlations in different futures markets. *The European Physical Journal B, 58(2), 207–220.* [CrossRef]

Baruník, J., & Křehlík, T. (2018). Measuring the frequency dynamics of financial connectedness and systemic risk. *Journal of Financial Econometrics, 16*(2), 271–296. [CrossRef]

Bollerslev, T. (1987). A conditionally heteroskedastic time series model for speculative prices and rates of return. *The Review of Economics and Statistics, 69*(3), 542–547. [CrossRef]

Calomiris, C. W., Cakir Melek, N., & Mamaysky, H. (2026). Big data meets the turbulent oil market. *Financial Analysts Journal, 82*(1), 35–59. [CrossRef]

Carchano, Ó., & Pardo, Á. (2009). Rolling over stock index futures contracts. *Journal of Futures Markets, 29*(7), 684–694. [CrossRef]

Chen, Y.-L., & Yang, J. J. (2024). Time-varying price discovery in regular and microbitcoin futures. *Journal of Futures Markets, 44*(1), 103–121. [CrossRef]

Chen, C., & Yu, D. (2025). The role of speculators in the crude oil futures market: Risk sharing or risk taking. *Journal of Futures Markets, 45(9), 1343–1360.* [CrossRef]

Clewlow, L., Kang, B., & Nikitopoulos, C. S. (2014). On the volatility of commodity futures prices. In R. Dieci, X.-Z. He, & C. Hommes (Eds.), *Nonlinear economic dynamics and financial modelling* (pp. 315–334). Springer. [CrossRef]

Conlon, T., Corbet, S., & Oxley, L. (2024). Investor sentiment, unexpected inflation, and Bitcoin basis risk. *Journal of Futures Markets, 44*(11), 1807–1831. [CrossRef]

Demiralay, S., Bayraci, S., & Gencer, H. G. (2019). Time-varying diversification benefits of commodity futures. *Empirical Economics, 56*(6), 1823–1853. [CrossRef]

Demiralay, S., Gencer, H. G., & Brauneis, A. (2025). Stock–commodity correlations, optimal hedging, and climate risks. *Journal of Futures Markets, 45*(10), 1693–1716. [CrossRef]

Dickey, D. A., & Fuller, W. A. (1979). Distribution of the estimators for autoregressive time series with a unit root. *Journal of the American Statistical Association, 74*(366a), 427–431. [CrossRef]

Diebold, F. X., & Yilmaz, K. (2009). Measuring financial asset return and volatility spillovers, with application to global equity markets. *The Economic Journal, 119*(534), 158–171. [CrossRef]

Diebold, F. X., & Yilmaz, K. (2012). Better to give than to receive: Predictive directional measurement of volatility spillovers. *International Journal of Forecasting, 28*(1), 57–66. [CrossRef]

Diebold, F. X., & Yilmaz, K. (2014). On the network topology of variance decompositions: Measuring the connectedness of financial firms. *Journal of Econometrics, 182*(1), 119–134. [CrossRef]

Dutta, A. (2025). Assessing the risk of Bitcoin futures market: New evidence. *Annals of Data Science, 12*(2), 481–497. [CrossRef]

Edwards, F. R., Hanley, K., Litan, R., & Weil, R. L. (2019). Crypto assets require better regulation: Statement of the Financial Economists Roundtable on crypto assets. *Financial Analysts Journal, 75*(2), 14–19. [CrossRef]

Engle, R. F. (1982). Autoregressive conditional heteroscedasticity with estimates of the variance of United Kingdom inflation. *Econometrica, 50*(4), 987–1007. [CrossRef]

Engle, R. F. (2002). Dynamic conditional correlation: A simple class of multivariate generalized autoregressive conditional heteroskedasticity models. *Journal of Business & Economic Statistics, 20*(3), 339–350. [CrossRef]

Erb, C. B., & Harvey, C. R. (2006). The strategic and tactical value of commodity futures. *Financial Analysts Journal, 62*(2), 69–97. [CrossRef]

Etienne, X., Li, B., & Liu, R. (2025). Detangling risk premiums: Common and idiosyncratic components of crude oil, corn, and ethanol futures. *Journal of Futures Markets, 45(9), 1409–1427.* [CrossRef]

French, K. R., & Roll, R. (1986). Stock return variances: The arrival of information and the reaction of traders. *Journal of Financial Economics, 17*(1), 5–26. [CrossRef]

Frino, A., Gaudiosi, R., Webb, R. I., & Zhou, Z. I. (2025). Price discovery in Bitcoin spot or futures? The jury is out. *Journal of Futures Markets, 45*(4), 269–288. [CrossRef]

Getmansky, M., Girardi, G., & Lewis, C. (2016). Interconnectedness in the CDS market. *Financial Analysts Journal, 72*(4), 62–82. [CrossRef]

Gorton, G., & Rouwenhorst, K. G. (2006). Facts and fantasies about commodity futures. *Financial Analysts Journal, 62*(2), 47–68. [CrossRef]

Grieb, T. (2015). Mean and volatility transmission for commodity futures. *Journal of Economics and Finance, 39*(1), 100–118. [CrossRef]

Hess, D., Huang, H., & Niessen, A. (2008). How do commodity futures respond to macroeconomic news? *Financial Markets and Portfolio Management, 22*(2), 127–146. [CrossRef]

Hoque, M. E., Bilgili, F., & Batabyal, S. (2023). What do we know about spillover between the climate change futures market and the carbon futures market? *Climatic Change, 176*(12), 166. [CrossRef]

Hornback, A. M., & Whaley, R. E. (2025). Spot Bitcoin ETFs: The struggle was worth it. *Financial Analysts Journal, 81*(2), 39–50. [CrossRef]

Jarque, C. M., & Bera, A. K. (1987). A test for normality of observations and regression residuals. *International Statistical Review, 55*(2), 163–172. [CrossRef]

Jensen, G. R., Johnson, R. R., & Washer, K. M. (2018). All that's gold does not glitter. *Financial Analysts Journal, 74*(1), 59–76. [CrossRef]

Karagiorgis, A., & Ballis, A. (2026). Time-varying skewness–kurtosis dynamics in Bitcoin markets. *Journal of Futures Markets, 46(8), 1440–1452.* [CrossRef]

Khan, N., Guesmi, K., Su, T., & Lucey, B. (2026). Connectedness across healthcare cryptocurrencies, DeFi, and NFTs tokens: Which global risk factors should be given more attention? *Journal of Futures Markets, 46(5), 878–903.* [CrossRef]

Koop, G., Pesaran, M. H., & Potter, S. M. (1996). Impulse response analysis in nonlinear multivariate models. *Journal of Econometrics, 74*(1), 119–147. [CrossRef]

Korolev, G. (2026). Facts and fantasies about DeFi: Lending, DEX, and derivatives. *Journal of Futures Markets, 46*(8), 1350–1379. [CrossRef]

Krückeberg, S., & Scholz, P. (2020). Decentralized efficiency? *Arbitrage in Bitcoin markets. Financial Analysts Journal, 76*(3), 135–152. [CrossRef]

Kwiatkowski, D., Phillips, P. C. B., Schmidt, P., & Shin, Y. (1992). Testing the null hypothesis of stationarity against the alternative of a unit root. *Journal of Econometrics, 54*(1–3), 159–178. [CrossRef]

Levine, A., Ooi, Y. H., Richardson, M., & Sasseville, C. (2018). Commodities for the long run. *Financial Analysts Journal, 74*(2), 55–68. [CrossRef]

Li, X., Tang, Y., Li, X., Zou, Z., & Xu, S. (2026). *Currency network dynamics and renminbi spillover effects in the Asia-Pacific region*. *International Journal of Finance & Economics*. Advance online publication. [CrossRef]

Liu, S., Lu, L., Liu, M., & Parker, R. (2026). Machine learning forecasts of tail-risk spillovers in carbon and energy markets. *Journal of Forecasting, 45(4), 1954–1984.* [CrossRef]

Ljung, G. M., & Box, G. E. P. (1978). On a measure of lack of fit in time series models. *Biometrika, 65*(2), 297–303. [CrossRef]

Lupu, R., & Popa, C. M. (2024). The efficiency of futures markets on cryptocurrencies. In L. Chivu, C. Ciutacu, V. Ioan-Franc, & J. V. Andrei (Eds.), *Constraints and opportunities in shaping the future: New approaches to economics and policy making* (pp. 271–282). Springer. [CrossRef]

Martens, M., & Poon, S.-H. (2001). Returns synchronization and daily correlation dynamics between international stock markets. *Journal of Banking & Finance, 25*(10), 1805–1827. [CrossRef]

Moutinho, V., Oliveira, H., Neves, M., & Monteiro, J. (2026). Risk transmission and co-movements between financial markets and commodity markets in the COVID-19 period. *International Journal of Finance & Economics*. Advance online publication. [CrossRef]

Nakajima, K. (2020). Commodity spot and futures prices under supply, demand, and financial trading: Single input–output model. *Asia-Pacific Financial Markets, 27*(1), 35–59. [CrossRef]

Niu, Z., Demirer, R., Suleman, M. T., & Zhang, H. (2024). Speculation, cross-market sentiment and the predictability of gold market volatility. *Journal of Behavioral Finance, 25*(3), 278–295. [CrossRef]

Page, S., & Panariello, R. A. (2018). When diversification fails. *Financial Analysts Journal, 74*(3), 19–32. [CrossRef]

Pan, M.-S., & Hsueh, L. P. (1998). Transmission of stock returns and volatility between the U.S. *and Japan: Evidence from the stock index futures markets. Asia-Pacific Financial Markets, 5*(3), 211–225. [CrossRef]

Pesaran, M. H., & Shin, Y. (1998). Generalized impulse response analysis in linear multivariate models. *Economics Letters, 58*(1), 17–29. [CrossRef]

Phillips, P. C. B., & Perron, P. (1988). Testing for a unit root in time series regression. *Biometrika, 75*(2), 335–346. [CrossRef]

Qin, S., & Lau, W.-Y. (2024). Extreme risk spillovers from US soybean futures market to China's soybean-linked

futures markets. *Journal of Futures Markets, 44*(11), 1735–1749. [CrossRef]

Ren, X., Xiao, S., Zhang, W., & Sun, X. (2025). Tail risk spillover of commodity futures markets. *Accounting & Finance, 65*(1), 109–141. [CrossRef]

Rezitis, A. N., Andrikopoulos, P., & Daglis, T. (2024). Assessing the asymmetric volatility linkages of energy and agricultural commodity futures during low and high volatility regimes. *Journal of Futures Markets, 44*(3), 451–483. [CrossRef]

Sayed, A., & Auret, C. (2019). Volatility transmission in maize futures markets of major exporters. *Investment Analysts Journal, 48*(3), 173–187. [CrossRef]

Sharma, U., & Karmakar, M. (2024). Asymptotic dependence and its impact on hedging effectiveness: An examination of stock, currency, and commodity futures. *Journal of Futures Markets, 44*(11), 1750–1786. [CrossRef]

Shynkevich, A. (2026). Trading periodicity and algorithmic divide in cryptocurrency markets. *Journal of Futures Markets, 46(5), 904–930.* [CrossRef]

Solibakke, P. B. (2015). Stochastic volatility models for the Brent oil futures market: Forecasting and extracting conditional moments. *OPEC Energy Review, 39*(2), 184–221. [CrossRef]

van Oordt, M. R. C., Stork, P. A., & de Vries, C. G. (2021). On agricultural commodities' extreme price risk. *Extremes, 24*(3), 531–563. [CrossRef]

Wang, Z., Yang, W., Ren, X., & Lu, Z. (2026). *Spillover effects of global commodities under VIX shocks: Evidence from dynamic quantile network model*. *International Journal of Finance & Economics*. Advance online publication. [CrossRef]

Wong, S. K., Chau, K. W., & Yiu, C. Y. (2007). Volatility transmission in the real estate spot and forward markets. *Journal of Real Estate Finance and Economics, 35*(3), 281–293. [CrossRef]

Wu, S., Chen, B., & Xiong, D. (2015). Topological properties of stock index futures based on network approach. In R. Zhang, Z. Zhang, K. Liu, & J. Zhang (Eds.), *LISS 2013: Proceedings of the 3rd International Conference on Logistics, Informatics and Service Science* (pp. 135–140). Springer. [CrossRef]

Yang, S., & Kwon, H. (2026). *Developing predictive and explainable models for cryptocurrency delistings: A case study of Binance exchange*. *Asia-Pacific Journal of Financial Studies*. Advance online publication. [CrossRef]

Zainudin, A. D., & Mohamad, A. (2023). Pandemic impact on the co-movement and hedging effectiveness of the global futures markets. *Investment Analysts Journal, 52*(2), 132–152. [CrossRef]

Zhou, L., & Li, J. (2026). Contagion of commodity futures price bubbles: Perspectives from futures-level sentiment contagion. *Journal of Economic Interaction and Coordination, 21*(1), 49–92. [CrossRef]

Genişletilmiş Özet

Amaç: Emtia vadeli işlem piyasaları son yirmi yılda giderek finansallaşırken, kripto paralar olağanüstü yüksek oynaklığa sahip ayrı bir varlık sınıfı olarak ortaya çıkmıştır. Bu iki piyasanın tek bir bütünleşik risk sisteminin parçaları mı olduğu yoksa büyük ölçüde ayrışık mı kaldığı, hem portföy çeşitlendirmesi hem de sistemik risk gözetimi açısından doğrudan sonuçları olan bir sorudur. Bu çalışma, altı emtia vadeli işlem sözleşmesi (altın, gümüş, bakır, WTI ham petrol, doğal gaz, buğday) ile dört kripto para (Bitcoin, Ethereum, XRP, Litecoin) arasındaki oynaklık bağlanmışlığını 2016–2026 döneminde ölçerek ve kritik olarak toplam bağlanmışlığı blok-içi ve bloklar-arası bileşenlerine ayrıştırarak bu soruyu yanıtlamaktadır.

Yöntem: Ortak işlem günlerinde eşleştirilen günlük ABD doları kapanış fiyatları, 25 Ağustos 2016 – 30 Haziran 2026 dönemini kapsayan 2.471 gözlemlik bir örneklem üretmektedir. Önce her seri için GARCH(1,1) modeliyle koşullu oynaklıklar tahmin edilmiş; ardından bu oynaklıklar üzerine on değişkenli bir VAR kurulmuş ve değişken sıralamasından bağımsız olan genelleştirilmiş öngörü hata varyansı ayrıştırmasından Diebold–Yılmaz bağlanmışlık ölçütleri hesaplanmıştır. Toplam, yönlü (yayma/alma), net ve net ikili bağlanmışlık raporlanmaktadır. Çalışmanın temel yöntemsel katkısı, toplam bağlanmışlığın dört blok bileşenine emtia-içi, kripto-içi, emtiadan kriptoya ve kriptodan emtiaya toplamı birebir tutan tam bir ayrıştırmasıdır. Dinamik bağlanmışlık 250 gözlemlik kayan pencerelerle izlenmiş; seçilmiş çiftler için DCC-GARCH, getiri düzeyinde tamamlayıcı kanıt olarak tahmin edilmiştir. Sağlamlık; öngörü ufku (5, 10, 20 gün), VAR gecikme uzunluğu (1, 2, 4, 6), kayan pencere genişliği (150, 200, 250, 300 gözlem), veri kaynağı ve takvim hizalaması, getiri frekansı, uç gözlemlerin işlenmesi, oynaklık ölçütü ve alt dönem boyutlarında on dört alternatif belirtimle sistematik biçimde sınanmıştır.

Bulgular: Sistemin toplam bağlanmışlığı %28,7'dir. Ancak blok ayrıştırması, bu toplamın %61,4'ünün kripto bloğunun, %34,9'unun emtia bloğunun kendi içinde gerçekleştiğini; bloklar arası aktarıma toplamın yalnızca %3,6'sının kaldığını ortaya koymaktadır (emtiadan kriptoya 0,42 puan; kriptodan emtiaya 0,62 puan). En büyük net yayıcılar doğal gaz (+20,4) ve Ethereum (+8,5) iken, en büyük net alıcı güvenli liman rolüyle tutarlı biçimde altındır (−18,7). Mutlak değerce en büyük sekiz net ikili bağlanmışlığın tamamı blok-içi çiftlerde gerçekleşmekte, listede tek bir emtia–kripto çifti bulunmamaktadır. Dinamik bağlanmışlık belirgin biçimde zaman-değişkendir (%24,3–66,8): ortalaması %39,3'tür ve COVID-19 salgınının küresel piyasaları vurduğu 2020'nin ilk yarısında %56,7'ye yükselmiştir. DCC tahminleri ayrışmayı getiri düzeyinde desteklemektedir: emtia–kripto koşullu korelasyonları, sıfıra yakın DCC a parametreleriyle (0,001–0,009) ortalama 0,040–0,123 düzeyinde düşük ve istikrarlı kalırken, blok-içi korelasyonlar bunun yaklaşık dokuz katıdır (altın–gümüş 0,784; Bitcoin–Ethereum 0,758). Ayrışma bulgusu sağlamdır: en cömert belirtimde (altı gecikme) dahi bloklar arası yayılım, toplam bağlanmışlığın %5,3'ünü aşmamakta; on dört alternatif belirtimin hiçbirinde blok-içi aktarımın baskınlığı bozulmamaktadır.

Sonuç ve Öneriler: Emtia vadeli işlem ve kripto para piyasaları oynaklık bakımından ayrışık kalmaktadır; iki piyasa farklı şok kaynaklarınca sürüklenmekte ve bu nedenle birbirlerine güçlü bir karşılıklı çeşitlendirme sunmaktadır. Çalışmanın başlıca yöntemsel uyarısı, toplam bağlanmışlık ölçütünün blok yapısını gizleyebildiğidir: %28,7'lik manşet değer orta düzeyde bütünleşme izlenimi verirken, blok ayrıştırması ayrışmaya işaret etmektedir. Aynı dikkat yönlü ölçütler için de geçerlidir. Bitcoin'in %52,6'lık yüksek yayma değeri, emtia piyasalarına oynaklık ihracını değil, kripto bloğu içindeki başat konumunu yansıtmaktadır. Uygulayıcılar açısından çeşitlendirme faydası gerçektir ancak sistemik stres dönemlerinde kısmen zayıflamaktadır; kripto varlıklar portföy bağlamında büyük ölçüde tek bir risk kümesi olarak ele alınmalıdır; 2,8–3,2 aralığında tahmin edilen Öğrenci-t serbestlik dereceleri ve bire dayanan oynaklık kalıcılığı göz önüne alındığında, kripto pozisyonları için riske maruz değer hesapları normallik varsayımına dayandırılmamalıdır. Düzenleyiciler açısından ise ayrışma iki yönlü okunmalıdır: kriptodan emtiaya bulaşma riski düşüktür, ancak kripto bloğunun kendi içindeki yüksek bağlanmışlık, sistemik riskin bu blok içinde yoğunlaştığını göstermektedir. Çalışmanın sınırlılıkları; iki piyasanın ortak bir işlem takvimi paylaşmamasını ve farklı saatlerde kapanmasını (etkisi sağlamlık bölümünde sınanmıştır), kripto tarafında vadeli sözleşme yerine spot fiyat kullanımını, koşullu oynaklığın iki aşamalı tahminini ve on varlıkla sınırlı kesiti içermektedir. Gelecek araştırmalar bu çerçeveyi frekans-alanı ve kantil bağlanmışlığa, düzenlenmiş kripto vadeli sözleşmelerine ve stablecoin'ler ile merkeziyetsiz finans jetonlarını da içeren daha geniş bir varlık kesitine genişletebilir.